University of Dundee

Mode of Action of the Natural Product Allicin in a Plant Model

Noll, Ulrike; Schreiber, Miriam; Hermanns, Monika; Mertes, Christopher A.; Slusarenko, Alan J.; Gruhlke, Martin C.H.

Citation for published version (APA):
Noll, U., Schreiber, M., Hermanns, M., Mertes, C. A., Slusarenko, A. J., & Gruhlke, M. C. H. (2022). Mode of Action of the Natural Product Allicin in a Plant Model: Influence on the Cytoskeleton and Subsequent Shift in Auxin Localization. *Applied Sciences*, *12*(22), [11470]. https://doi.org/10.3390/app122211470

Article

Mode of Action of the Natural Product Allicin in a Plant Model: Influence on the Cytoskeleton and Subsequent Shift in Auxin Localization

Ulrike Noll [1,2], Miriam Schreiber [1,3], Monika Hermanns [1], Christopher A. Mertes [1], Alan J. Slusarenko [1,2] and Martin C. H. Gruhlke [1,2,*]

1   Department of Plant Physiology, RWTH Aachen University, Worringer Weg 1, 52074 Aachen, Germany
2   Society for Natural Product and Drug Research, Lukasstrasse 1, 52070 Aachen, Germany
3   College of Life Sciences, University of Dundee, Division of Plant Science, Errol Road, Invergowrie, Dundee DD2 5DA, UK
*   Correspondence: martin.gruhlke@genawif.com; Tel.: +49-241-98091551

Abstract: Allicin is a defense substance produced by garlic cells when they are injured. It is a redox-active thiosulfinate showing redox-activity with a broad range of dose-dependent antimicrobial and biocidal activity. It is known that allicin efficiently oxidizes thiol-groups, and it has been described as a redox toxin because it alters the redox homeostasis in cells and triggers oxidative stress responses. Allicin can therefore be used as a model substance to investigate the action of thiol-specific prooxidants. In order to learn more about the effect of allicin on plants, we used pure synthetized allicin, and studied the influence of allicin on organelle movement in Tradescantia fluminensis as a cytoskeleton-dependent process. Furthermore, we investigated cytoplasmic streaming in sterile filaments of Tradescantia fluminensis, organelle movement using transgenic Arabidopsis with organelle-specifics GFP-tags, and effects on actin and tubulin in the cytoskeleton using GFP-tagged lines. Tubulin and actin were visualized by GFP-tagging in transgenic lines of *Arabidopsis thaliana* to visualize the influence of allicin on the cytoskeleton. Since auxin transport depends on recycling and turnover of the PIN protein involving cytoskeletal transport to and from the membrane localization sites, auxin distribution in roots was investigated using of transgenic PIN1–GFP, PIN3–GFP, DR5–GFP and DII–VENUS Arabidopsis reporter lines. Allicin inhibited cytoplasmic streaming in T. fluminensis, organelle movement of peroxi-somesperoxisomes, and the Golgi apparatus in a concentration-dependent manner. It also destroyed the correct root tip distribution of auxin, which probably contributed to the observed inhibition of root growth. These observations of the disruption of cytoskeleton-dependent transport processes in plant cells add a new facet to the mechanism of action of allicin as a redox toxin in cells.

Keywords: allicin; redox; tradescantia; arabidopsis; cytoskeleton; auxin; mode of action

1. Introduction

Actin and tubulin are major structural components of the cytoskeleton, and their polymerization and depolymerization are important, amongst other things, for cytoplasmic streaming and intracellular trafficking [1]. Soon after the discovery of actin, it was shown that oxidizing agents not only inhibited the polymerization of globular actin, but also depolymerized actin filaments [2]. The importance of sulfhydryl groups for protoplasmic streaming in plant cells was reported in 1964 by Abe [3] who showed the effect of the specific thiol-trapping reagent *p*-chloromercuribenzoate in bringing cytoplasmic streaming to a standstill in the internodal cells of *Nitella flexilis*, the leaf cells of *Elodea densa*, the root hair cells of *Hydrocharis morsus ranae*, and the stamen hair cells of *Tradescantia reflexa*. Elements of the cytoskeleton are known to be highly sensitive to oxidation [4,5], and redox-mediated

posttranslational modifications of the cytoskeleton affect polymerization [6,7]. The redox regulation of actin and tubulin dynamics is now a well characterized phenomenon [8–10].

Allicin from garlic is the most prominent sulfur-containing bioactive compound in freshly damaged garlic tissue [11,12]. It oxidizes thiol-groups in a thiol-disulfide-exchange-like manner, leading to S-thioallylated adducts [13–17]. Since allicin is a strongly antimicrobial compound with a broad-spectrum of activity, it has the potential for application in agricultural pest control [18–22]. Allicin's degradation products, primarily polysulfanes, ajoenes, and vinyldithiins, can also show biological activity and can be active as antimicrobial components. The effect of these sulfur-containing components in allelopathic interactions with other organisms can be of importance, as is observed in particular for wild garlic (*Allium ursinum* L.), to which is attributed the exudation of sulfur-containing secondary metabolites [23].

In animal cells, it was shown that allicin, which acts as a "redox-toxin" [13], affects the integrity and function of the cytoskeleton [24]. It was reported that 0.5 µM of allicin preferentially affected the tubulin cytoskeleton, while the actin cytoskeleton was a minor target (ibid.). However, at a higher 25 µM concentration of allicin, the actin cytoskeleton was also reported to be disrupted [25]. Furthermore, 16 cytoskeletal proteins were shown to be S-thioallylated by 100 µM of allicin in human Jurkat cells within 10 min of exposure [26].

The actin cytoskeleton is of particular importance for the correct polar transport of auxin in relation to PIN efflux carrier recycling [27–29]. Auxin also exerts an influence on the regulation of actin turnover [30]. The high redox sensitivity of actin is probably significant for the observation that auxin transport is related to the state of the total cellular glutathione pool, which is the most important thiol-based redox buffer of the cell [31]. Thus, treatment of *Arabidopsis thaliana* seedlings with buthionine sulphoximine (BSO), a specific inhibitor of glutathione biosynthesis, led to a clear concentration-dependent inhibition of root growth and a loss of the auxin efflux carriers PIN1, PIN2, and PIN7, as well as the consequent destruction of the correct auxin distribution in the root tip (ibid.). This observation correlates with the finding that mutants in glutathione biosynthesis formed shortened roots, such as was seen in the weak allele mutants *pad2* and *cad2* of the *Arabidopsis thaliana GSH1* gene, which had reduced glutathione levels [32]. Mutants of the strong rml1 (root meristemless) allele of *GSH1* were almost unable to produce glutathione, could not maintain the root apical meristem, and consequently could not form a root [33,34].

Due to the need to understand the phytotoxicity of allicin with regard to its possible use in organic farming, as well as the allelopathic effects of these substances, we are interested in understanding the molecular causes of the effects of allicin on plants. It has already been reported that allicin inhibits *Arabidopsis thaliana* primary and lateral root growth in a concentration-dependent manner [35,36]. In the work reported here, we analyzed the effect of allicin, applied as a solution of chemically synthesized pure allicin, on the cytoskeleton and consequent cytoskeleton-dependent cellular processes like cytoplasmic streaming, organelle movement, and auxin distribution, which may have led to the root growth-inhibiting effects of allicin.

2. Materials and Methods

2.1. Plant material and cultivation

Tradescantia fluminensis VELL was cultivated in the greenhouse. For the induction of flowering, the plants were grown in nutrient-poor soil.

Mutants and different GFP-tagged *Arabidopsis thaliana* lines used in this study are listed in Table 1. The plants were grown in solid Hoagland-medium (1 mM $CaNO_3$; 5.1 mM KNO_3; 0.5 mM $MgSO_4$; 0.5 mM $MgCl_2$; 0.13 mM $(NH_4)H_2PO_4$; 30 µM NH_3NO_3; 31 µM NaOH; 22 µM EDTA-Iron-Sodium Salt; 9.7 µM BH_3O_3; 22 µM $FeSO_4$; 2 µM $MnSO_4$; 0.31 µM $ZnCl_2$, 0.21 µM $CuSO_4$; 0.14 µM Na_2MoO_4; 86 nM $Co(NO_3)_2$, containing 8 g/L of plant agar (Duchefa, Haarlem, The Netherlands). After stratification for two days at 4 °C, the seedlings were grown under long day conditions (16 h light, 8 h dark; 22 °C) for two days before treatment.

Table 1. Mutants and transgenic *Arabidopsis thaliana* lines used in this study.

Mutant	Phenotype	Reference
ABD2–GFP	GFP-fusion protein with actin binding protein ABD2 allows visualization of actin cytoskeleton	[37]
Tubulin–GFP	GFP-fusion with beta-tubulin allows visualization of tubulin cytoskeleton	[38]
GFP–PTS	Fusion of GFP with peroxisomal targeting sequence allows visualization of peroxisomes	[39]
pad2	weak GSH1 allele, homozygote has ~30% GSH content of the wild type	[40]
axr1-12	No auxin perception	[41]
aux1-2	Lack of auxin importer AUX1-2.	[41]
DR5–GFP	GFP expression dependent on the auxin-responsive DR5 promoter.	[42]
DII–VENUS	Degradation of the fluorescent protein depending on the presence of auxin	[43]

2.2. Synthesis of Allicin and Quantification of Allicin

The chemical synthesis of allicin was conducted as described previously [13]. The purity of the chemically synthesized allicin was >95% (ibid.).

2.3. Measurement of Protoplasmic Streaming

As a measure of the influence of allicin on protoplastic flow, the time was recorded for cytoplasmic flow to cease following exposure to allicin. For this purpose, individual sterile flower filaments were plucked off with tweezers and placed under a microscope as a water preparation. To prevent the specimen from being crushed, the cover glass was slightly raised by small amounts of plasticine at the corners. Treatment with allicin or garlic juice was carried out by using a filter paper to draw off the water under the coverslip and replace it with allicin solutions of the appropriate concentration. In the same way, the allicin solution was exchanged for distilled water for the regeneration experiments. Microscopy was carried out at 400× magnification using transmitted light microscopy. Separate staining was not necessary.

2.4. Confocal Laser Scan Microscopy

For GFP-visualization, a Confocal Laser Scan Microscope (TCS SP1, Leica GmbH, Wetzlar, Germany) was used with an excitation wavelength of 488 nm and an emission filter of 500–550 nm. For microscopy, a 63× water immersion objective was used and processed with ImageJ (http://rsbweb.nih.gov/ij, last accessed on 18 August 2018).

For analysis of the cytoskeleton, two-day-old seedlings were used; the seedlings were placed on a slide in water or in an allicin solution of the indicated concentration. The analysis was carried out after 30 min. For the PIN and auxin localization study, seedlings were placed in Hoagland medium containing a concentration of 2 mM. The seedlings were incubated for 24 h under short day conditions (22 °C, 16 h dark, 8 h light) before microscopic analysis.

2.5. Growth Assays

Arabidopsis thaliana seeds were surface sterilized with ethanol and spread with a toothpick onto solid Hoagland medium. Plates were stored at 4 °C for two days for stratification before incubation at 22 °C for an additional two days under long day conditions (16 h light/8 h dark). After this time, seedlings were carefully transferred with forceps to Hoagland medium plates containing allicin at a final concentration of 0.5 mM and fur-

ther incubated under these conditions. Root length was measured at day zero and after three days.

2.6. Statistics

Statistical analyses were carried out using the program SigmaStat. Data were tested for statistical significance using a multivariate data analysis (ANOVA) with a significance level of $p < 0.05$. The data were first tested for normal distribution to allow for valid application of the statistical tests.

3. Results and Discussion

3.1. Protoplasmic Streaming in Tradescantia Fluminensis VELL

As a model system for the influence of allicin on the cytoskeleton, we chose the sterile hyaline filaments from the flower of *T. fluminensis* (shown in Figure 1A–C). The time that elapsed until cytoplasmic streaming ceased after exposure to allicin solutions of various concentrations was considered as a measure of the relative activity of allicin on the cytoskeleton. Particles carried in the cytoplasmic stream were observed to have locomotion (Figure 1D,E). Soon after the hyaline filaments of *T. fluminensis* were exposed, the flow slowed down and stopped entirely after a certain time, which was dependent on the allicin concentration. As the concentration of allicin increased, the time required for the protoplasmic flow to come to a standstill decreased (Figure 1D). While a concentration of 0.5 mM of allicin led to a cessation of protoplasmic flow after approx. 13 min, a treatment with 4 mM of allicin led to a complete cessation of protoplasmic flow after approx. 2 min (Figure 1D).
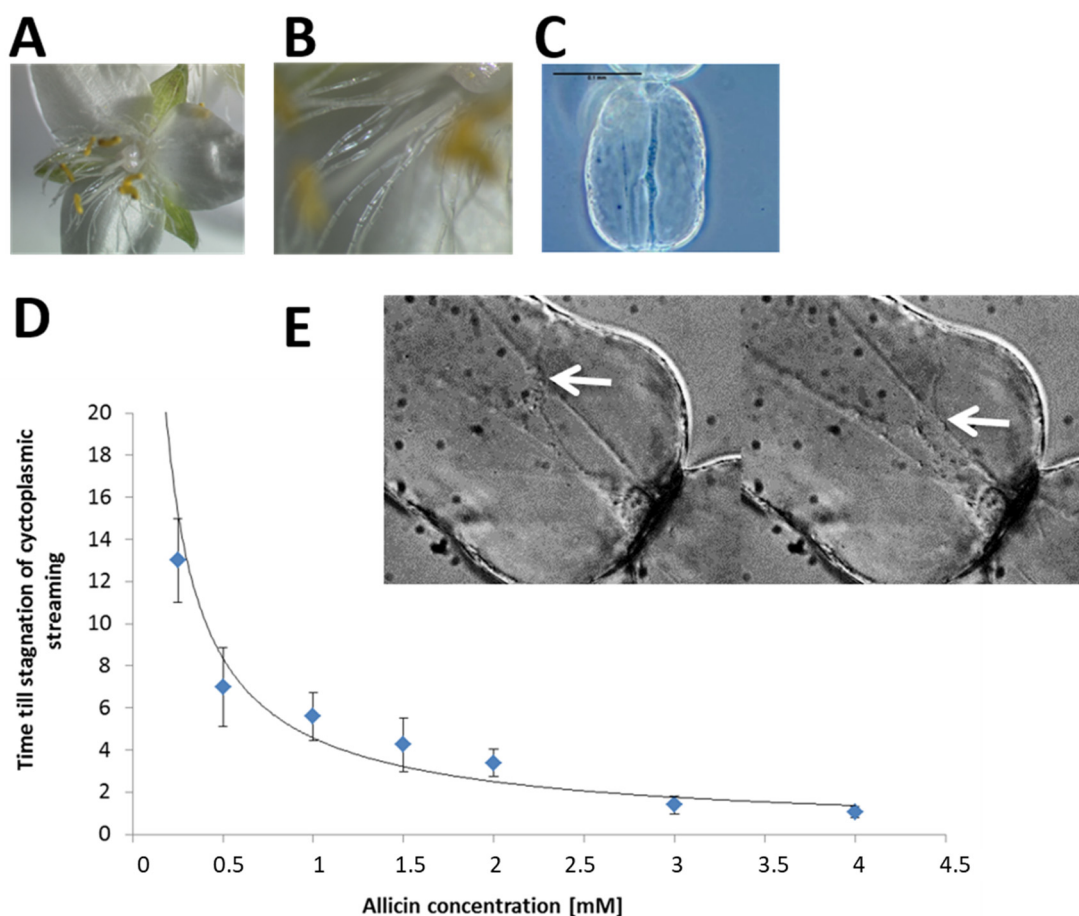

Figure 1. (**A–C**) Sterile filaments in the flower of *Tradescantia fluminensis* are made up of hyaline cells and are well suited to observe protoplasmic streaming. The scale bar in (**C**) = 0.1 mm (**D**) Allicin led

to a concentration- and time-dependent decrease in protoplasmic flow. The time that elapsed at a certain concentration of allicin until protoplasmic flow stopped was measured, showing a correlation between the allicin concentration and the time that elapsed until flow stopped. (**E**) Movement of structures in the protoplasmic stream, in this case a fork in cytoplasmic strands, could be used to measure the protoplasmic streaming.

A further observation for 5, 10, and 30 min after treatment showed that, in the presence of allicin, no new onset of protoplasmic disturbance was observed.

3.2. The Effect of Allicin on the Protoplasmic Streaming Was Partially Reversible

In the following experiments, it was investigated as to whether the effect of allicin was reversible by washing out the allicin. Filaments of Tradescantia were treated with allicin with a final concentration of 0.25 mM. After cytoplasmic flow stopped, the allicin solution was washed by capillary suction with filter paper that drew in pure water at the coverslip edge to exchange the bathing solution. After about 12 min, protoplasmic flow began again in isolated cells, although at a slower rate than before allicin treatment (not shown). Thus, it can be concluded that the inhibition of protoplasmic flow by allicin can be reversible after a certain regeneration phase; at a concentration higher than 0.25 mM allicin, this reversal did not occur even after a long observation period (>30 min).

3.3. Influence of Allicin on the Movement of Peroxisomes in Leaves

Since the movement of organelles, such as peroxisomes, also takes place within the framework of protoplasmic flow, an *Arabidopsis thaliana* line was used whose peroxisomes were tagged with GFP [39]. This made their movement traceable. Leaves of this *Arabidopsis thaliana* line were infiltrated by vacuum infiltration, with either water as a control treatment or an allicin solution of the indicated concentration, and the movement of the organelles was observed under a confocal laser scanning microscope (Figure 2A,B). While in the control, it was clearly indicated by observing the curved trail of peroxisome movements between the arrows that the peroxisomes moved substantially over the 10 min observation period (Figure 2A), in the sample infiltrated with 4 mM of allicin, movement of the peroxisomes was not observed (Figure 2B).
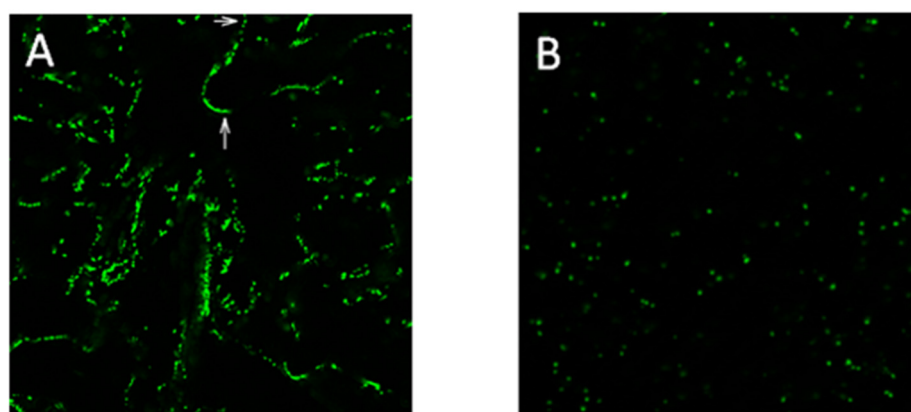

Figure 2. Movement of GFP-labelled peroxisomes in *Arabidopsis thaliana* treated with either (**A**) water as a control or (**B**) 4 mM allicin. The images show a stack of 20 images each, taken 30 s apart.

3.4. Allicin Inhibits Primary- and Lateral Root Growth and Root Hair Development

The morphology of *Arabidopsis thaliana* wild type Col-0 seedlings germinated for two days and exposed to 0.5 mM of allicin was very reminiscent of the morphology of the rml1 mutant [33]. The roots of wild type Col-0 ceased growing in the presence of allicin, while the shoot axis appeared to be largely unaffected and developed normally (Figure 3A). Compared to the untreated control, the roots of plants exposed to allicin

were generally much shorter and showed no lateral roots or root hairs. The prooxidant cumene hydroperoxide also led to a similarly shortened root (Figure 3B). Root growth in the pad2 mutant was also similarly inhibited by allicin and cumene hydroperoxide under the conditions tested (Figure 3B).
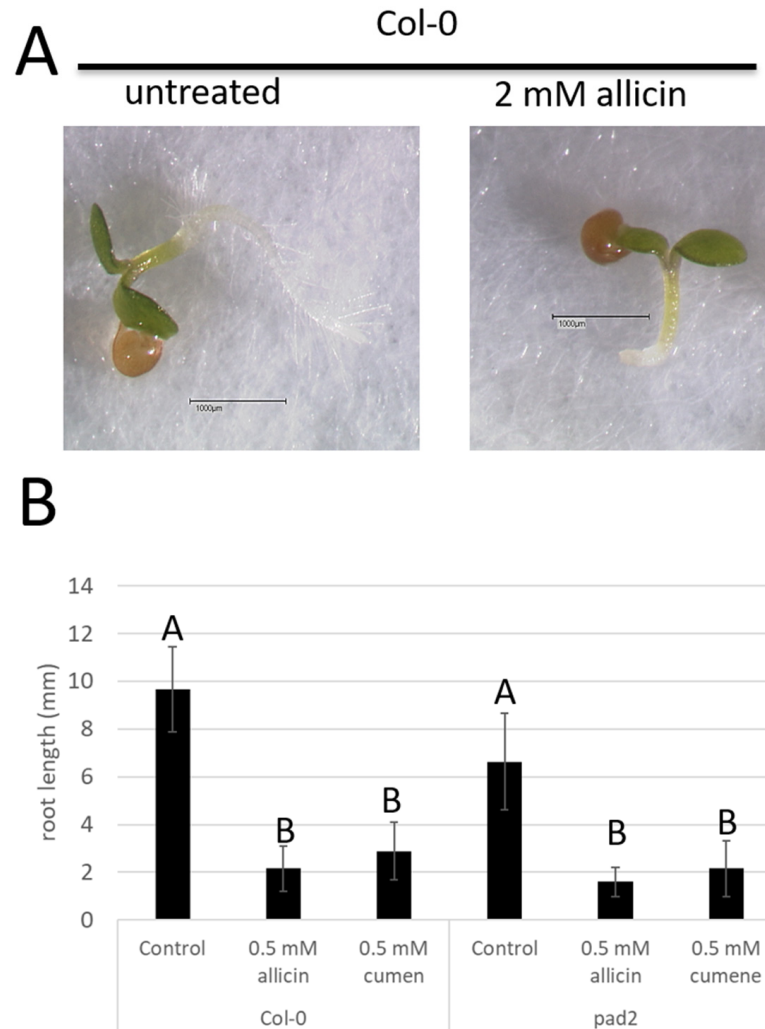

Figure 3. Allicin inhibited primary root growth and root hair development. Seeds were germinated for two days on filter paper discs, which were then lifted and transferred to fresh medium containing allicin (**A**) or cumene hydroperoxide at the stated concentrations. (**B**) Wild type Col-0 was compared to the GSH-deficient *pad2* mutant. The scale bars = 1 mm. N = 20, experiment was repeated three times with similar results. The letters A, B above the respective graph columns indicate statistical differences as determined by ANOVA analysis.

3.5. Effect of Allicin on Actin- and Tubulin Cytoskeleton in Arabidopsis thaliana

To understand in more detail how allicin affects root development and whether this is associated with the putative effect on the cytoskeleton that was observed in Tradescantia, *Arabidopsis thaliana* lines were used whose actin or tubulin filaments were visualized with by beta-tubulin–GFP fusion [38] and GFP–actin-binding protein expression [37].

Confocal microscopy of the actin cytoskeleton clearly showed typical filamentous structures in the root of the untreated control (Figure 4A). After exposure to 2 mM of allicin for 24 h, the filamentous structures were destroyed; instead, GFP aggregate structures were visible at the margins of the cells. Allicin thus destroyed the integrity of the actin cytoskeleton in the roots of *Arabidopsis thaliana*.
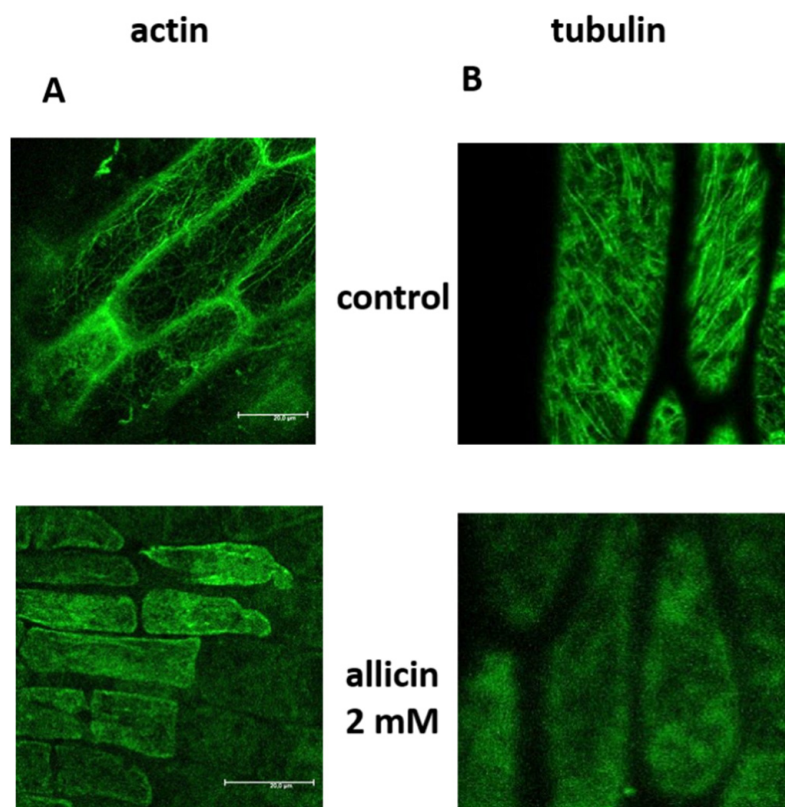
Figure 4. Effect of 2 mM allicin on the actin and tubulin cytoskeleton after exposure for 24 h. While controls exposed to water only showed a typical filamentous structure of both the actin and tubulin, they were completely dissolved after 24 h exposure to allicin. (**A**) shows the influence of allicin on the actin cytoskeleton, (**B**) shows the influence of allicin from the plexus of tubulin in the cell.

In addition to the actin cytoskeleton, the tubulin cytoskeleton was also examined in an analogous manner. Here, too, the typical filament pattern was seen in the untreated control; treatment with allicin resulted in the dissolution of these filament structures and the diffuse fine-particulate distribution of GFP fluorescence, in contrast to the aggregate formation observed for the actin.

3.6. Effect of Allicin on Auxin Distribution PIN Localization

The cytoskeleton fulfils a wide variety of tasks in the cell and is involved, among other things, in transport processes in the cell. In order to investigate the influence of cytoskeletal integrity—here primarily concerning actin—on important cellular transport processes, we chose the localization of PIN proteins, whose localization is crucial for regulated auxin transport in tissues. Again, GFP-tagged versions of the proteins, in this case PIN1 and PIN3, were used to track their localization in vivo. In addition, the expression of the constructs was under the respective native promoter, so that the localization of the expression could also be followed at the tissue level.

In the untreated control, the PIN1 showed expression mainly in the region of the central cylinder (Figure 5A); at the cellular level, the strongest fluorescence was observed on the basipetal side of the cell. The exposure to allicin with a concentration of 2 mM led to a complete loss of this clear localization pattern, and GFP fluorescence was weakly distributed throughout the cell (Figure 5B). This corresponded exactly to the observations made by Koprivova during treatment with BSO, which suggests that allicin was also active here via the glutathione pool [31].
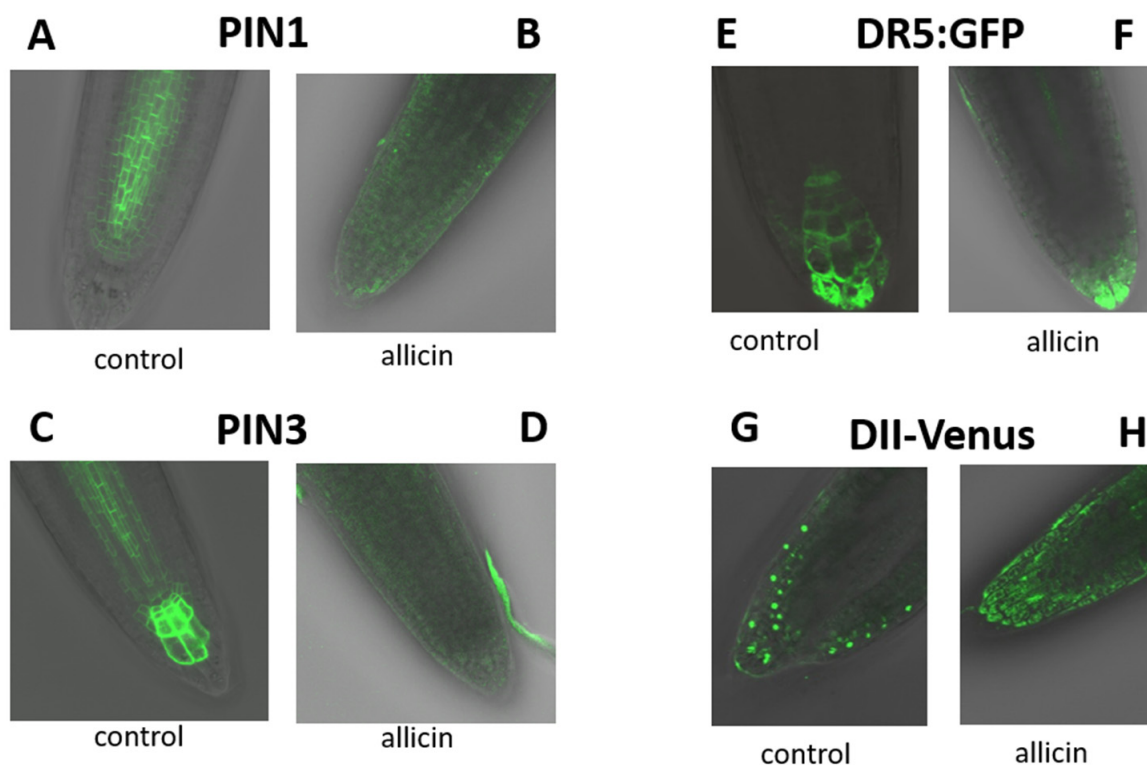
Figure 5. Influence of allicin on the localization of PIN1 and PIN3 proteins and on auxin distribution in the root tip. (**A**) While the localization of PIN1 in the control was restricted to the central cylinder, a diffuse localization of PIN1 is seen in (**B**) allicin-exposed plants. (**C**) The localization of PIN3 in the control is seen in the central cylinder and in the meristematic zone of the root tip, but under allicin exposure (**D**) the localization of PIN 3 protein was also diffuse. This was also reflected in the localization of auxin. In control plants, where GFP expression was under the auxin-responsive DR5 promoter, a typical distribution of auxin is seen in the root tip, meristematic and quiescent zone (**E**), whereas this clear localization was abolished under allicin exposure (**F**). The detection of auxin distribution in the root by means of DII–VENUS indicated in a complementary way that no auxin was present where the fluorescent protein was observed, because auxin led to the degradation of the protein. Accordingly, in the control (**G**), fluorescence is seen in the marginal areas of the root, but not in the meristematic and quiescent zone, whereas under allicin exposure, fluorescence is observed everywhere in the cells (**H**). All treated samples were exposed to 2 mM allicin for 24 h.

In contrast to the PIN1, the localization of the PIN3 was also found in the area of the cortex, but it was more prominent in the area of the root apical meristem. Again, fluorescence was strongest at the basipetal end of the cell (Figure 5C).

As observed with the PIN1, complete disruption of the PIN localization had also occurred with PIN3 by treatment with 2 mM of allicin. The GFP signal, which indicated the localization of the PIN1 protein, was diffusely present at both the cellular and tissue levels (Figure 5D). These results exactly mirrored the effects of the GSH1 inhibitor buthione sulfoximine (BSO) on PIN distribution [31]. BSO led to a reduction in cellular GSH levels, and this mirrored the result of allicin titrating out and oxidizing the GSH pool [13].

3.7. Effect of Allicin on Auxin Distribution

Based on the observation that allicin destroyed the localization of PIN proteins, and because PIN proteins are essential for the directional transport of auxin, the final aim was to investigate whether the aberrant localization of auxin occurred after allicin treatment. Two independent methods based on fluorescent proteins were used to check the localization of allicin. The DR5–GFP reporter system was based on the fact that auxin induced the activity

of the DR5 promoter and thus drove GFP expression. GFP fluorescence thus indexed the presence of auxin.

Untreated *Arabidopsis thaliana* roots showed a clear localization of auxin around the quiescent zone of the root apical meristem, in the central cylinder and in the epidermal layers of the root (Figure 5E). Treatment with allicin resulted in the localization of GFP fluorescence being restricted to the root apex; auxin-dependent expression of GFP was no longer found in the quiescent and division zone of the root apex (Figure 5F). This showed that allicin caused a clear redistribution of auxin localization at the root tip.

As an alternative method to detect the localization of auxin at the tissue level, the DII–VENUS construct was used, in which a "fast maturing" form of yellow-fluorescent protein (YFP) was expressed in frame with an IAA protein under the control of a constitutive promoter. Because IAA proteins are degraded in the presence of auxin, a lack of fluorescence of the VENUS protein would indicate a high concentration of auxin, whereas a strong fluorescence of the protein would indicate a low concentration of auxin. The results obtained by means of DII–VENUS corresponded to the statements we also perceived with DR5–GFP. While the control showed that auxin was present in the root meristem area, the distribution was diffuse after allicin exposure (Figure 5G).

3.8. Effect of Allicin on Mutants Impaired in Auxin Homeostasis and Signaling

Because we observed an effect on auxin distribution and PIN localization after allicin treatment (Figure 5), we investigated the effects of allicin on the auxin transport mutant aux1-2 and the auxin-resistant mutant axr1-12 in comparison to wild type Col-0. Whereas the PIN proteins are functional in auxin efflux at the basal cell pole, the AUX1 protein transports auxin into the cell from the apoplast at the apical pole.

The Col-0 wild type showed that its exposure to 0.5 mM of allicin led to a significantly shortened root. The aux1-2 mutant root length, which already had a significantly shortened root in the control compared to the Col-0, was not further affected by the presence of allicin, i.e., this mutant showed a degree of allicin resistance (Figure 6A) and this suggests that the root phenotype we observed with allicin may have been dependent upon auxin over-accumulating to supraoptimal levels and that inhibited root growth. The axr1-12 mutant, on the other hand, showed no significant change in root length phenotype compared to the wild type in the control, but treatment with allicin caused the roots to be shortened, but to a much lesser extent than in the Col-0 control. This suggests that the influence of allicin on auxin transport was partly responsible for the observation that the roots did not grow as well under allicin exposure (Figure 6B). Possibly, another auxin receptor could have partially complemented the phenotype of axr1-12. To test this hypothesis, Col-0 and axr1-12 mutants were exposed to 20 μM of cytochalasin, which led to disruption of the actin cytoskeleton. As a control, it was examined whether the solvent DMSO at the concentration used (1% *v/v*) would lead to an effect, which was not the case. While the Col-0 wild type showed significantly shortened roots after treatment with cytochalasin, the axr1-12 mutant did not, which suggested that it was disruption of the actin cytoskeleton which altered auxin localization. Accordingly, a mutant that was not an auxin receptor mutant showed no phenotype in terms of root length upon destruction of the actin cytoskeleton. These results suggest that the effect allicin has on root development correlates, at least in part, with its influence on auxin distribution in the root, which are dependent upon allicin's effects on the cytoskeleton.
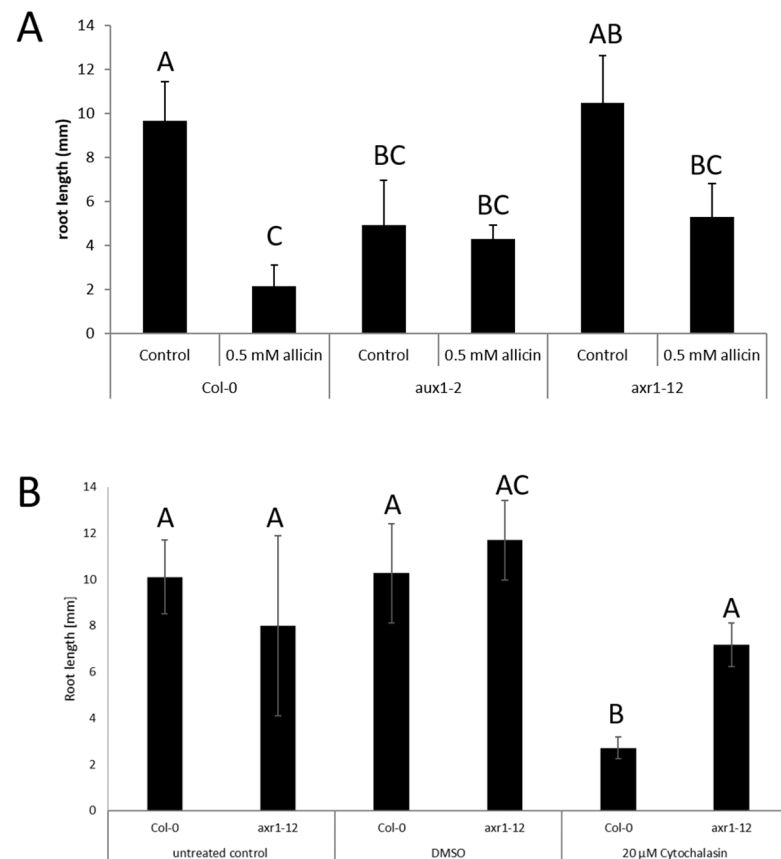
Figure 6. Influence of allicin (**A**) and cytochalasin (**B**) on *aux1-2* and *axr1-12* mutants. (N = 20) The experiments were repeated three times with similar results. Mutants were compared against the underlying Col-0 wild type; treatment with DMSO served as a solvent control. The letters A–C above the respective graph columns indicate statistical differences as determined by ANOVA analysis.

4. Conclusions

The thiosulfinate allicin directly affects the cytoskeleton through its thiol-oxidizing properties. In the model system *Tradescantia fluminensis*, it was shown that the protoplasm flow was stopped. GFP-tagged cytoskeletal components revealed that the direct disruption of both actin and tubulin filaments also occurred. Since the localization of the phytohormone auxin, which is crucial for root development, is regulated by the orientation of PIN channels and crucially depends on the functionality of the cytoskeleton, we tested the hypothesis of whether, on the one hand, PIN channels showed an altered localization and, on the other hand, auxin was localized in an altered manner as a result. Both could be shown by GFP probes. This resulted in a shortening of the roots due to auxin mislocalization in the growth zone. Thus, it was clear that oxidative stress in roots led to a shortening of the roots, which was due to an influence on the cytoskeleton integrity and subsequent mislocalization of the auxin. This has far reaching environmental relevance, far beyond the study of the effect of allicin as a model substance.

Data Availability Statement: The original data presented in this study are available upon request.

Conflicts of Interest: The authors declare no conflict of interest.

References

1. Allen, N.S.; Allen, R.D. Cytoplasmic Streaming in Green Plants. *Annu. Rev. Biophys. Bioeng.* **1978**, *7*, 497–526. [CrossRef] [PubMed]
2. Feuer, G.; Molnar, F.; Pettko, E.; Straub, F.B. Studies on the composition and polymerization of actin. *Hung. Acta Physiol.* **1948**, *1*, 150–163. [PubMed]
3. Abe, S. The effect of p-chloromercuribenzoate on rotational protoplasmic streaming in plant cells. *Protoplasma* **1964**, *58*, 483–492. [CrossRef]
4. Farah, M.E.; Amberg, D.C. Conserved actin cysteine residues are oxidative stress sensors that can regulate cell death in yeast. *Mol. Biol. Cell.* **2007**, *18*, 1359–1365. [CrossRef] [PubMed]
5. Farah, M.E.; Sirotkin, V.; Haarer, B.; Kakhniashvili, D.; Amberg, D.C. Diverse protective roles of the actin cytoskeleton during oxidative stress. *Cytoskeleton* **2011**, *68*, 340–354. [CrossRef] [PubMed]
6. Johansson, M.; Lundberg, M. Glutathionylation of beta-actin via a cysteinyl sulfenic acid intermediary. *BCM Biochem.* **2007**, *8*, 26. [CrossRef]
7. Wang, J.; Boja, E.S.; Tan, W.; Tekle, E.; Fales, H.M.; English, S.; Mieyal, J.J.; Chock, P.B. Reversible glutathionylation regulates actin polymerization in A431 cells. *J. Biol. Chem.* **2001**, *276*, 47763–47766. [CrossRef]
8. Wilson, C.; Terman, J.R.; Gonzalez-Billault, C.; Ahmed, G. Actin filaments—A target for redox regulation. *Cytoskeleton* **2016**, *73*, 577–595. [CrossRef]
9. Landino, L.M.; Robinson, S.H.; Skreslet, T.E.; Cabral, D.M. Redox modulation of tau and microtubule-associated protein-2 by the glutathione/glutaredoxin reductase system. *Biochem. Biophys. Res. Commun.* **2004**, *323*, 112–117. [CrossRef] [PubMed]
10. Livanos, P.; Galatis, B.; Apostolakos, P. The interplay between ROS and tubulin cytoskeleton in plants. *Plant Signal Behav.* **2014**, *9*, e28069. [CrossRef] [PubMed]
11. Cavallito, C.J.; Bailey, J.H. Allicin, the Antibacterial Principle of *Allium sativum* L. Isolation, Physical Properties and Antibacterial Action. *J. Am. Chem. Soc.* **1944**, *66*, 1950–1951. [CrossRef]
12. Block, E. The Organosulfur Chemistry of the Genus *Allium*—Implications for the Organic Chemistry of Sulfur. *Angew. Chem. Int. Edit.* **1992**, *31*, 1135–1178. [CrossRef]
13. Gruhlke, M.C.H.; Portz, D.; Stitz, M.; Anwar, A.; Schneider, T.; Jacob, C.; Schlaich, N.L.; Slusarenko, A.J. Allicin disrupts the cell's electrochemical potential and induces apoptosis in yeast. *Free Rad. Biol. Med.* **2010**, *49*, 1916–1924. [CrossRef] [PubMed]
14. Gruhlke, M.C.H.; Nwachukwu, I.; Arbach, M.; Anwar, A.; Noll, U.; Slusarenko, A.J. Allicin from Garlic, Effective in Controlling Several Plant Diseases, is a Reactive Sulfur Species (RSS) that Pushes Cells into Apoptosis. In *Modern Fungicides and Antifungal Compounds VI*; Dehne, H.W., Deising, H.B., Gisi, U., Kuck, K.H., Russell, P.E., Lyr, H., Eds.; Deutsche Phytomedizinische Gesellschaft: Braunschweig, Germany, 2011; pp. 325–330.
15. Miron, T.; Listowsky, I.; Wilchek, M. Reaction mechanisms of allicin and allyl-mixed disulfides with proteins and small thiol molecules. *Eur. J. Med. Chem.* **2010**, *45*, 1912–1918. [CrossRef]
16. Pinto, J.T.; Krasnikov, B.F.; Cooper, A.J.L. Redox-sensitive proteins are potential targets of garlic-derived mercaptocysteine derivatives. *J. Nutr.* **2006**, *136*, 835–841. [CrossRef] [PubMed]
17. Winkler, G.; Iberl, B.; Knobloch, K. Reactivity of Allicin and its Transformation Products with Sulfhydryl Groups, Disulfide Groups, and Human Blood. *Planta Med.* **1992**, *58*, 665. [CrossRef]
18. Auger, J.; Arnault, I.; Diwo-Allain, S.; Ravier, M.; Molia, F.; Pettiti, M. Insecticidal and fungicidal potential of Allium substances as biofumigants. *Agroindustria* **2004**, *3*, 5–8.
19. Freeman, F.; Kodera, Y. Garlic Chemistry: Stability of S(2-Propenyl) 2-Propene-1-sulfinothioate (Allicin) in Blood, Solvents, and Simulated Physiological Fluids. *J. Agric. Food Chem.* **1995**, *43*, 2332–2338. [CrossRef]
20. Portz, D.; Koch, E.; Slusarenko, A.J. Effects of garlic (*Allium sativum* L.) juice containing allicin on *Phytophthora infestans* (Mont.deBary) and on downy mildew of cucumber caused by *Pseudoperonospora cubensis* (Berk. & M.A. Curtis) Rostovzev. *Eur. J. Plant Pathol.* **2008**, *122*, 197–206.
21. Slusarenko, A.J.; Patel, A.; Portz, D. Control of plant diseases by natural products: Allicin from garlic as a case study. *Eur. J. Plant Pathol.* **2008**, *121*, 313–322. [CrossRef]
22. Slusarenko, A.J.; Anwar, A.; Portz, D.; Noll, U. Garlic—A Call to Arms. *Outlooks Pest Manag.* **2011**, *22*, 83–86. [CrossRef]
23. Block, E. *Garlic and Other Alliums—The Lore and the Science*; Royal Society of Chemistry: Cambridge, UK, 2010.
24. Prager-Khoutorsky, M.; Goncharov, I.; Rabinkov, A.; Mirelman, D.; Geiger, B.; Bershadsky, A.D. Allicin inhibits cell polarization, migration and division via its direct effect on microtubules. *Cytoskeleton* **2007**, *64*, 321–337. [CrossRef]
25. Sela, U.; Ganor, S.; Hecht, I.; Brill, A.; Miron, T.; Rabinkov, A.; Wilchek, M.; Mirelman, D.; Lider, O.; Hershkoviz, R. Allicin inhibits SDF-1α-induced T cell interactions with fibronectin and endothelial cells by down-regulating cytoskeleton rearrangement, Pyk-2 phosphorylation and VLA-4 expression. *Immunology* **2004**, *111*, 391–399. [CrossRef]

26. Gruhlke, M.C.H.; Antelmann, H.; Bernhardt, J.; Kloubert, V.; Rink, L.; Slusarenko, A.J. The human allicin-proteome: S-thioallylation of proteins by the garlic defence substance allicin and its biological effects. *Free Radic. Biol. Med* **2019**, *131*, 144–153. [CrossRef]

27. Vieten, A.; Sauer, M.; Brewer, P.B.; Friml, J. Molecular and cellular aspects of auxin-transport-mediated development. *Trends Plant Sci.* **2007**, *12*, 160–168. [CrossRef]

28. Nick, P.; Han, M.-J.; An, G. Auxin Stimulates Its Own Transport by Shaping Actin Filaments. *Plant Physiol.* **2009**, *151*, 155–167. [CrossRef]

29. Rahman, A.; Bannigan, A.; Sulaman, W.; Pechter, P.; Blancaflor, E.B.; Baskin, T.I. Auxin, actin and growth of the *Arabidopsis thaliana* primary root. *Plant J.* **2007**, *50*, 514–528. [CrossRef] [PubMed]

30. Zou, M.; Ren, H.; Li, J. An Auxin Transport Inhibitor Targets Villin-Mediated Actin Dynamics to Regulate Polar Auxin Transport. *Plant Physiol.* **2019**, *181*, 161–178. [CrossRef] [PubMed]

31. Koprivova, A.; Mugford, S.; Kopriva, S. Arabidopsis root growth dependence on glutathione is linked to auxin transport. *Plant Cell Rep.* **2010**, *29*, 1157–1167. [CrossRef]

32. Bashandy, T.; Guilleminot, J.; Vernoux, T.; Caparros-Ruiz, D.; Ljung, K.; Meyer, Y.; Reichheld, J.-P. Interplay between the NADP-Linked Thioredoxin and Glutathione Systems in Arabidopsis Auxin Signaling. *Plant Cell* **2010**, *22*, 376–391. [CrossRef] [PubMed]

33. Cheng, J.C.; Seeley, K.A.; Sung, Z.R. RML1 and RML2, Arabidopsis Genes Required for Cell Proliferation at the Root Tip. *Plant Physiol.* **1995**, *107*, 365–376. [CrossRef] [PubMed]

34. Vernoux, T.; Wilson, R.C.; Seeley, K.A.; Reichheld, J.P.; Muroy, S.; Brown, S.; Maughan, S.C.; Cobbett, C.S.; Montagu, M.V.; Inzé, D.; et al. The ROOT MERISTEMLESS1/CADMIUM SENSITIVE2 gene defines a glutathione-dependent pathway involved in initiation and maintenance of cell division during postembryonic root development. *Plant Cell* **2000**, *12*, 97–110. [CrossRef] [PubMed]

35. Borlinghaus, J.; Albrecht, F.; Gruhlke, M.; Nwachukwu, I.; Slusarenko, A. Allicin: Chemistry and Biological Properties. *Molecules* **2014**, *19*, 12591–12618. [CrossRef] [PubMed]

36. Leontiev, R.; Hohaus, N.; Jacob, C.; Gruhlke, M.C.H.; Slusarenko, A.J. A Comparison of the Antibacterial and Antifungal Activities of Thiosulfinate Analogues of Allicin. *Sci. Rep.* **2018**, *8*, 6763. [CrossRef] [PubMed]

37. Voigt, B.; Timmers, A.C.J.; Amaj, J.S.; Müller, J.; Baluska, F.; Menzel, D. GFP-FABD2 fusion construct allows in vivo visualization of the dynamic actin cytoskeleton in all cells of *Arabidopsis* seedlings. *Eur. J. Cell Biol.* **2005**, *84*, 595–608. [CrossRef]

38. Ueda, K.; Matsuyama, T.; Hashimoto, T. Visualization of microtubules in living cells of transgenic *Arabidopsis thaliana*. *Protoplasma* **1999**, *206*, 201–206. [CrossRef]

39. Mano, S.; Nakamori, C.; Hayashi, M.; Kato, A.; Kondo, M.; Nishimura, M. Distribution and Characterization of Peroxisomes in Arabidopsis by Visualization with GFP: Dynamic Morphology and Actin-Dependent Movement. *Plant Cell Physiol.* **2002**, *43*, 331–341. [CrossRef]

40. Glazebrook, J.; Ausubel, F.M. Isolation of phytoalexin-deficient mutants of *Arabidopsis thaliana* and characterization of their interactions with bacterial pathogens. *Proc. Natl. Acad. Sci. USA* **1994**, *91*, 8955–8959. [CrossRef]

41. Timpte, C.; Lincoln, C.; Pickett, F.B.; Turner, J.; Estelle, M. The AXR1 and AUX1 genes of *Arabidopsis* function in separate auxin-response pathways. *Plant J.* **1995**, *8*, 561–569. [CrossRef]

42. Friml, J.; Vieten, A.; Sauer, M.; Weijers, D.; Schwarz, H.; Hamann, T.; Offringa, R.; Jürgens, G. Efflux-dependent auxin gradients establish the apical–basal axis of *Arabidopsis*. *Nature* **2003**, *426*, 147–153. [CrossRef]

43. Brunoud, G.; Wells, D.M.; Oliva, M.; Larrieu, A.; Mirabet, V.; Burrow, A.H.; Beeckman, T.; Kepinski, S.; Traas, J.; Bennett, M.J.; et al. A novel sensor to map auxin response and distribution at high spatio-temporal resolution. *Nature* **2012**, *482*, 103–106. [CrossRef] [PubMed]